Nanopores in the ventral scales of *Bitis rubida* and *Bitis armata* cause white venters

KM Samaun Reza[1,2], Luisa Maren Borgmann[1], Dmitry Busko[1], Junchi Chen[2], Hans Gunstheimer[1,3], Richard Thelen[1], Guillaume Gomard[4], Uli Lemmer[1,2], Hendrik Hölscher[1,*]

[1]*Institute of Microstructure Technology, Karlsruhe Institute of Technology (KIT), Hermann-von-Helmholtz Platz 1, 76344 Eggenstein-Leopoldshafen, Germany*
[2]*Light Technology Institute (LTI), Karlsruhe Institute of Technology (KIT), Engesserstrasse 13, 76131 Karlsruhe, Germany*
[3]*Nanosurf AG, Gräubernstrasse 14, 4410 Liestal, Switzerland*
[4]*Carl Zeiss AG, ZEISS Innovation Hub @ KIT, Hermann-von-Helmholtz Platz 6, 76344 Eggenstein-Leopoldshafen, Germany*

Date: 5 April 2025

Email: `hendrik.hoelscher@kit.edu`

Keywords: Snake scales, structural white, wideband scattering, thermoregulation

Abstract: Recent studies speculated that some snakes developed white venters to avoid overheating caused by highly radiative soil and rocks. Here, we present the scale-embedded porous nanostructures through which some snake species of the genus *Bitis* achieve such whiteness. Our analysis reveals nanopores causing scattering underneath the external surface of the white ventral scales of *Bitis rubida* and *Bitis armata*. Such nanopores are not present in the scales of *Bitis parviocula, Bitis arietans*, and *Bitis rhinoceros* that appear transparent or translucent to the naked eye. White ventral scales with nanopores reflect up to 40% of light in the visible regime. The reflection, however, decreases for longer wavelengths and drastically reduces in the infrared. In contrast, a much lower, almost constant reflection around 8% between 250 nm and 2500 nm is observed for the transparent or translucent ventral scales without nanopores. Our study demonstrates that some snake species of the genus *Bitis* utilize a light scattering network of nanopores underneath their external surfaces to create white ventral scales.

Introduction

Numerous ecological and evolutionary factors lead to the colouration in organisms through evolution [1]. This colouration might be caused by pigmentation, structural colours or both [2–4]. The resulting broad variety of colours assists animals in camouflage [5–9], communication

[10,11], mating [12], and thermoregulation [13–15]. In general, body temperature is directly affected by the absorption and reflection of electromagnetic radiation [16]. Especially, cold-blooded squamates rely on this property for thermoregulation [17].

In general, multifunctional macromolecules like melanin play a significant role in controlling the brightness of the skin [18]. The dark optical appearance of melanin helps to absorb solar radiation [16,19]. Many studies on squamates discuss their dorsal scale colouration (see, *e.g*., Refs. [14,20–23]). Martínez-Freiria *et al.* [24], for example, studied the relation between the degree of pigmentation of the zigzag pattern on the dorsal scales of Eurasian vipers and environmental variables such as solar radiation, elevation, and latitude. They concluded that the dorsal scales with high melanin content help snakes absorb more sunlight to ensure thermoregulation within the snake's body.

Although several studies discussed the colouration of dorsal scales, only a few focused on the ventral colouration of the squamates [25–28]. In 2015 and 2016, Moreno Azócar *et al*. [29,30] concluded that species living closer to the Equator are most likely to have brighter venters. Later, Goldenberg *et al*. [31] reported on the reflecting venters of snakes, comparing the scales of 126 species. They applied a comparative approach to investigate the macro-evolutionary processes involved in developing ventral brightness. Their study concludes that vipers living on hot and highly radiative and superficially conductive substrates develop less melanic ventral scales because the colour of the venter influences body temperature via the thermal transfer with the ground [30,31]. Conversely, the species living in lower energy radiation zones tend to have darker ventral scales, providing a thermal advantage. These studies already indicate that the colouration of the ventral snake scales might depend on the habitat of ectotherms. However, they did not examine the optical mechanism through which the respective snake species achieve such white ventral scales.

Here, we present a study on the structural and optical properties of the shed skin of ventral scales of snakes that appear white or transparent/translucent to the naked eye. Five species of the genus *Bitis* [32] were used as samples for this study. The ventral scales of the Red Adder (*Bitis rubida*), the Southern Adder (*Bitis armata*), the Ethiopian Viper (*Bitis parviocula*), the Puff Adder (*Bitis arietans*), and the West African Gaboon Viper (*Bitis rhinoceros*) are examined to reveal the physical origin of the whiteness of ventral scales. The surface analysis of these scales by atomic force microscopy (AFM) reveals shallow nanoscale features on the scale's surfaces of all five species. However, scanning electron microscopy (SEM) of the ventral scale cross-section revealed numerous nanopores underneath the external surfaces of the reflecting scales of *B. rubida* and *B. armata*. In opposite to that, such nanopores are not observed in the transparent or translucent scales of *B. parviocula, B. arietans*, and *B. rhinoceros*. As it was speculated that snakes utilize the colouration of their venter for thermoregulation, the scales were optically characterized in the wavelength range of 250 nm to 2500 nm. High reflection is observed in the visible and near-infrared light for the porous ventral scales of *B. rubida* and *B. armata*. Low constant reflection of 8%, on the other hand, is observed on the scales of *B. parviocula, B. arietans*, and *B. rhinoceros* in the entire spectrum of consideration. Therefore, we conclude that these nanopores scatter light in the visible and near-infrared regime, leading to white ventral scales. This enhanced reflection in such a broadband spectrum might help snakes to enhance their thermoregulatory properties on their ventral side.

Results

The left panel of Figure 1 displays photographs of the examined snake species and ventral white scales of *B. rubida* (Figure 1A), *B. armata* (Figure 1B) and transparent or translucent scales of *B. parviocula* (Figure 1C), *B. arietans* (Figure 1D), and *B. rhinoceros* (Figure 1E). The moulted ventral scales of the snakes, taken from the belly of the respective snake species, were placed on white paper with a printout of our university logo. In this way, the optical properties of the scales can be easily assessed by the naked eye. The printout cannot be seen through the reflecting ventral scales of *B. rubida* and *B. armata*. However, it can be easily spotted through the transparent or translucent ventral scales of *B. parviocula, B. arietans*, and *B. rhinoceros*.

As mentioned in the introduction, it was speculated in previous studies [29–31] that various reptiles developed white ventral bellies for thermoregulation. A white venter caused by white scales seems fortunate for the examined snakes to avoid overheating. Therefore, we studied the optical response of the scales of *B. rubida, B. armata, B. parviocula, B. arietans*, and *B. rhinoceros* in the wavelength range of 250 nm to 2500 nm (right panel of Figure 1).

A more or less constant total reflectance of around 8% is recorded on the ventral scales of *B. rhinoceros, B. arietans*, and *B. parviocula* in the range from 250 nm to 2500 nm. Accordingly, we observe a transmittance which increases sharply from the UV to values of about 90% for wavelength larger than 400 nm. However, as it might be expected by the optical impression already, a much higher reflectance and lower transmittance is observed on the ventral scales of the two other species. For *B. rubida*, the reflectance is about 30% in the lower range of the visible regime and increases continuously until it reaches a maximum of about 40% close to 500 nm. For increasing wavelengths, however, the total reflection decreases again and reduces to values of 20% at 2000 nm. The shape of the spectrum of *B. armata* is the same, but the overall reflectance values are about 10% lower. The transmittance for *B. rubida* as well as *B. armata* is about zero in the UV and increases continuously till it reaches a plateau in the infrared.

The comparison of the five spectra reveals that the total reflection of the white scales is much larger as for the transparent/translucent scales for all wavelengths under consideration. Especially in the near-infrared and even in the near ultraviolet (300 nm to 400 nm), the white scales of *B. rubida* and *B.armata* reflect significant parts of the electromagnetic spectrum.

To understand the mechanism through which these scales produce such a high reflection, we compare the topography and the inner structure of the scales imaged by AFM and SEM in Figure 2. A continuous ridge-like structure is observed on the surface of the scales of *B. rubida* (Figure 2A) and *B. armata* (Figure 2B). The ridges found on the scales of *B. rubida* are about 700 nm to 800 nm in width and around 1.7 µm to 2 µm on the scales of *B. armata*. The height of the ridges is around 100 nm for both species. Spike-like microfibrils are found on the scales of *B. parviocula* (Figure 2C) and *B. rhinoceros* (Figure 2E). The microfibrils are oriented in head to tail direction of the snakes' bodies. The AFM images in Figure 2C and E are oriented such that the head points toward the right side of the images. The height and periodicity of these microfibrils found on the scales of *B. parviocula* are in the range of 80 nm to 100 nm and 5 µm to 6 µm. The geometric values observed on the scales of *B. rhinoceros* are in the range of 40 nm to 50 nm and 7 µm to 8 µm, respectively. The surface found on the ventral side of *B. arietans* (Figure 2D) features a different structure with pits with a depth of around 15 nm to 30 nm and a diameter of 200 nm to 300 nm. Such pits were also observed on the scales of other species [33,34]. This topographical analysis reveals shallow nanostructures on the ventral scales of the investigated snake species. However, considering previous studies, we assume that snakes develop such nanoscale features to optimize their locomotion [35–42]. Such shallow nanostructures do not cause white, reflecting ventral scales.

Therefore, we cut the scales and imaged the resulting cross-sections by SEM. The resulting images show that the ventral scales of all examined species are multi-layered. In the first layer directly underneath the external surface of *B. rubida*, we observe a spongy layer with numerous nanopores. These nanopores are found in the upper 20-25 µm thick region of the top layer. Further magnification of these porous regions reveals that the embedded nanopores have neither a regular shape nor a pattern. They are about 0.5 µm to 1 µm in length and 0.25 µm to 0.5 µm in width. In the cross-section images, numerous nanopores are also found under the external surface of the white scales of *B. armata*. In both cases, the nanopores are closed structures without an opening to the outside. Consequently, we did not observe a colour-change when wetting the scales with water or index-matching liquid. However, such nanopores were not observed in the transparent or translucent scales of *B. parviocula, B. arietans*, and *B. rhinoceros* (see the zoom into the amorphous structure in Figure 2C).

To conclude, the metrological analysis reveals that nanopores are found in the white scales of *B. rubida* and B. *armata* while an amorphous structure without pores is found in the transparent or translucent scales of *B. parviocula, B. arietans*, and *B. rhinoceros*. This observation indicates that the nanopores scatter light to develop white ventral scales in some snake species. The overall results prove that the total reflectance of the porous ventral scales of *B. armata* and B. *rubida* is quite high in the visible and near-infrared regimes. However, the total reflectance is much lower for the amorphous ventral scales of *B. rhinoceros, B. arietans*, and *B. parviocula*. This result is conclusive evidence that high reflection is associated with the interaction of visible and near-infrared light with the nanopores found under the external surface.

Discussion and Conclusion

In the aforementioned studies [29–31], it was already discussed that many snake species develop a white reflecting venter. These species are mostly found in the equatorial region or hot and highly radiative and superficially conductive substrates. It was concluded that the reflecting venters facilitate such species in reducing heat absorption. Our experimental results are in accordance with these studies. Furthermore, our characterization identifies the optical structure through which some snakes achieve white-coloured scales, which assists their thermoregulation.

High reflection is observed on the ventral scales of *B. rubida* and B. *armata* where numerous nanopores were found underneath the external surfaces, but low reflection is measured on the amorphous scales of *B. parviocula, B. arietans*, and *B. rhinoceros*. This indicates that nanopores underneath the external surface interact with electromagnetic waves to reflect visible and near-infrared light. This high reflection in the visible and near-infrared regime indicates that these scales absorb less heat.

Surface topography analysis showed a ridge-like structure on the ventral scales of *B. rubida* and *B. armata*. These nanoscale ridges are quite shallow. Microfibril like patterning is observed on the ventral scales of *B. parviocula* and *B. rhinoceros*. Such structures are often found on the ventral scales of snake species [36]. Numerous pits are found on the ventral surface of *B. arietans*. It is widely accepted that such nanostructures on the ventral scales assist snakes in locomotion [35–41]. The ridge-like structure observed on the white scales does not interact with light to develop such optical properties, as similar structures can be observed on many other snakes without white venters. In the cross-section of ventral scales, numerous nanopores are observed in the white scales of *B. rubida* and *B. armata* underneath their external surfaces. However, such nanopores are not present in the transparent or translucent scales of *B. parviocula, B. arietans*, and *B. rhinoceros*.

We, therefore, conclude that these nanopores cause significant light scattering for a wide range of wavelengths. The same scattering principle was developed by beetles and birds, which utilize porous structures in their scales and feathers, respectively (see, *e.g.*, Refs. [43–45] and references therein). In summary, the white ventral scales of *B. rubida* and *B. armata* apply the same physical principle as beetles and birds so that they achieve whiteness through nanopores within an upper layer of their scales.

Methods

Snake Species: The surface topology, internal structure, and optical properties of the shed skin of ventral scales of five African vipers were analysed. Among them, the Red Adder (*Bitis rubida*) as well as the Southern Adder (*Bitis armata*) are only found in South Africa while the Ethiopian Viper (*Bitis parviocula*) originates from Ethiopia. The Puff Adder (*Bitis arietans*) is found in South Africa and other African countries. The West African Gaboon Viper (*Bitis rhinoceros*) is endemic to West Africa. According to Barlow *et al*. [32], this selection of *Bitis* species covers several types of habitats. As described in Ref. [32], the habitat of *B. rubida* and *B. armata* is lowland and montane rocky or gravely grassland, karroid and sclerophyllous scrub; *B. parviocula* and *B. rhinoceros* live in tropical and montane forest; while *B. arietans* lives in open savanna, grassland, and karroid scrub absent from forests and deserts. The moulted skins from captive snakes were collected by G. Gomard thanks to the contribution of different snake keepers (see Acknowledgments). Temperature (21 °C – 23 °C) and humidity (50% — 70%) were well controlled during storage and measurements of all samples.

Optical Spectroscopy: The total transmittance and reflectance spectra of the ventral scales were determined using a Cary 7000 spectrophotometer with an integrating sphere (DRS attachment, Agilent, USA). Unpolarized light was used to measure spectral properties, shining incoming light beams on the outer surfaces of the moulted snake scales close to normal incidence. The measured spectrum range was set to 250 to 2500 nm with a spectral resolution of ≈ 1 nm and a beam spot diameter of about 2 mm. This spectroscopy range covers most of the solar spectrum. The NIST calibrated Spectralon® diffuse reflectance standard (Labsphere, USA) was used to define a reference reflection.

Atomic Force Microscopy: To conduct a topological analysis of the scales' surface by atomic force microscope (AFM, Dimension Icon, Bruker), the scales were cut into small pieces. Two-component glue (UHU End-fest, UHU GmbH & Co. KG) was used to attach the samples to a glass slide for AFM imaging. The prepared samples were carefully cleaned with pressured air. Afterward, the samples were imaged in tapping mode utilizing rectangular silicon cantilevers (All-in-One-Al, Budget Sensors, Type C) as sensors.

Scanning Electron Microscopy: Scanning electron microscopy (SEM, SUPRA 60 VP, Zeiss, Germany) was applied for imaging the cross-sections of ventral scales. For that, the samples were carefully cut into pieces with a sharp razor blade and sputtered with a thin silver layer. The imaging was conducted with an acceleration voltage of 5 kV and the detector was placed at a working distance of 5 to 7 mm.

Supplemental

The supplemental shows a collection of photos displaying and cites references describing the venters of the examined snakes of the genus *Bitis*.

References

1. Endler JA, Westcott DA, Madden JR, Robson T. 2005 Animal Visual Systems and the Evolution of Color Patterns: Sensory Processing Illuminates Signal Evolution. *Evolution* **59**, 1795–1818. (doi:10.1554/04-669.1)

2. Parker AR. 2000 515 million years of structural colour. *J Opt. A* **2**, R15–R28. (doi:10.1088/1464-4258/2/6/201)

3. Vinther J, Briggs DEG, Clarke J, Mayr G, Prum RO. 2010 Structural coloration in a fossil feather. *Biol Lett* **6**, 128–131. (doi:10.1098/rsbl.2009.0524)

4. McNamara ME, Briggs DEG, Orr PJ, Noh H, Cao H. 2012 The original colours of fossil beetles. *Proc. R. Soc. B.* **279**, 1114–1121. (doi:10.1098/rspb.2011.1677)

5. Mäthger LM, Denton EJ, Marshall NJ, Hanlon RT. 2009 Mechanisms and behavioural functions of structural coloration in cephalopods. *J. R. Soc. Interface.* **6**, S149–S163. (doi:10.1098/rsif.2008.0366.focus)

6. Wilts BD, Michielsen K, Kuipers J, De Raedt H, Stavenga DG. 2012 Brilliant camouflage: photonic crystals in the diamond weevil, *Entimus imperialis*. *Proc. R. Soc. B.* **279**, 2524–2530. (doi:10.1098/rspb.2011.2651)

7. Norris KS, Lowe CH. 1964 An Analysis of Background Color-Matching in Amphibians and Reptiles. *Ecology* **45**, 565–580. (doi:10.2307/1936109)

8. Allen JJ, Mäthger LM, Barbosa A, Hanlon RT. 2009 Cuttlefish use visual cues to control three-dimensional skin papillae for camouflage. *J Comp Physiol A* **195**, 547–555. (doi:10.1007/s00359-009-0430-y)

9. Cuthill IC *et al.* 2017 The biology of color. *Science* **357**, 470. (doi:10.1126/science.aan0221)

10. Kemp DJ, Herberstein ME, Grether GF. 2012 Unraveling the true complexity of costly color signaling. *Behavioral Ecology* **23**, 233–236. (doi:10.1093/beheco/arr153)

11. Vukusic P, Sambles JR, Lawrence CR, Wootton RJ. 1999 Quantified interference and diffraction in single Morpho butterfly scales. *Proc. R. Soc. B.* **266**, 1403–1411. (doi:10.1098/rspb.1999.0794)

12. Loyau A, Gomez D, Moureau B, Théry M, Hart NS, Jalme MS, Bennett ATD, Sorci G. 2007 Iridescent structurally based coloration of eyespots correlates with mating success in the peacock. *Behavioral Ecology* **18**, 1123–1131. (doi:10.1093/beheco/arm088)

13. Schultz TD, Hadley NF. 1987 Structural Colors of Tiger Beetles and Their Role in Heat Transfer through the Integument. *Physiol Zool* **60**, 737–745. (doi:10.1086/physzool.60.6.30159990)

14. Tanaka K. 2007 Thermal biology of a colour-dimorphic snake, *Elaphe quadrivirgata*, in a montane forest: do melanistic snakes enjoy thermal advantages? *Biol J Linn Soc* **92**, 309–322. (doi:10.1111/j.1095-8312.2007.00849.x)

15. Smith KR, Cadena V, Endler JA, Porter WP, Kearney MR, Stuart-Fox D. 2016 Colour change on different body regions provides thermal and signalling advantages in bearded dragon lizards. *Proc. R. Soc. B.* **283**, 20160626. (doi:10.1098/rspb.2016.0626)

16. Clusella Trullas S, Van Wyk JH, Spotila JR. 2007 Thermal melanism in ectotherms. *J Therm Biol* **32**, 235–245. (doi:10.1016/j.jtherbio.2007.01.013)

17. Christian KA, Tracy CR. 1981 The effect of the thermal environment on the ability of hatchling Galapagos land iguanas to avoid predation during dispersal. *Oecologia* **49**, 218–223. (doi:10.1007/BF00349191)

18. Cordero RJB, Casadevall A. 2020 Melanin. *Curr. Biol.* **30**, R142–R143. (doi:10.1016/j.cub.2019.12.042)

19. Geen MRS, Johnston GR. 2014 Coloration affects heating and cooling in three color morphs of the Australian bluetongue lizard, Tiliqua scincoides. *J Therm Biol* **43**, 54–60. (doi:10.1016/j.jtherbio.2014.04.004)

20. Jackson JF, Ingram W, Campbell HW. 1976 The Dorsal Pigmentation Pattern of Snakes as an Antipredator Strategy: A Multivariate Approach. *Am Nat* **110**, 1029–1053. (doi:10.1086/283125)

21. Wüster W *et al.* 2004 Do aposematism and Batesian mimicry require bright colours? A test, using European viper markings. *Proc. R. Soc. Lond. B* **271**, 2495–2499. (doi:10.1098/rspb.2004.2894)

22. Allen WL, Baddeley R, Scott-Samuel NE, Cuthill IC. 2013 The evolution and function of pattern diversity in snakes. *Behavioral Ecology* **24**, 1237–1250. (doi:10.1093/beheco/art058)

23. Clause AG, Becker RN. 2015 Temperature Shock as a Mechanism for Color Pattern Aberrancy in Snakes. *Herpetol Notes* **8**, 331–334.

24. Martinez-Freiria F, Toyama KS, Freitas I, Kaliontzopoulou A. 2020 Thermal melanism explains macroevolutionary variation of dorsal pigmentation in Eurasian vipers. *Sci Rep* **10**, 16122. (doi:10.1038/s41598-020-72871-1)

25. Ressel S, Schall JJ. 1989 Parasites and showy males: malarial infection and color variation in fence lizards. *Oecologia* **78**, 158–164. (doi:10.1007/BF00377151)

26. Morrison RL, Rand MS, Frost-Mason SK. 1995 Cellular Basis of Color Differences in Three Morphs of the Lizard *Sceloporus undulatus erythrocheilus*. *Copeia* **1995**, 397. (doi:10.2307/1446903)

27. Stuart–Fox DM, Ord TJ. 2004 Sexual selection, natural selection and the evolution of dimorphic coloration and ornamentation in agamid lizards. *Proc. R. Soc. Lond. B* **271**, 2249–2255. (doi:10.1098/rspb.2004.2802)

28. Langkilde T, Boronow KE. 2012 Hot Boys Are Blue: Temperature-Dependent Color Change in Male Eastern Fence Lizards. *J. Herpetol.* **46**, 461–465. (doi:10.1670/11-292)

29. Moreno Azócar DL, Perotti MG, Bonino MF, Schulte JA, Abdala CS, Cruz FB. 2015 Variation in body size and degree of melanism within a lizards clade: is it driven by latitudinal and climatic gradients? *J Zool* **295**, 243–253. (doi:10.1111/jzo.12193)

30. Moreno Azócar DL, Bonino MF, Perotti MG, Schulte JA, Abdala CS, Cruz FB. 2016 Effect of body mass and melanism on heat balance in *Liolaemus* lizards of the *goetschi* clade. *J Exp Biol* , jeb.129007. (doi:10.1242/jeb.129007)

31. Goldenberg J, D'Alba L, Bisschop K, Vanthournout B, Shawkey MD. 2021 Substrate thermal properties influence ventral brightness evolution in ectotherms. *Commun Biol* **4**, 26. (doi:10.1038/s42003-020-01524-w)

32. Barlow A, Wüster W, Kelly CMR, Branch WR, Phelps T, Tolley KA. 2019 Ancient habitat shifts and organismal diversification are decoupled in the African viper genus *Bitis* (Serpentes: Viperidae). *J Biogeogr* **46**, 1234–1248. (doi:10.1111/jbi.13578)

33. Campbell AL, Bunning TJ, Stone MO, Church D, Grace MS. 1999 Surface Ultrastructure of Pit Organ, Spectacle, and Non Pit Organ Epidermis of Infrared Imaging Boid Snakes: A Scanning Probe and Scanning Electron Microscopy Study. *J Struct Biol* **126**, 105–120. (doi:10.1006/jsbi.1999.4121)

34. Arrigo MI, De Oliveira Vilaca LM, Fofonjka A, Srikanthan AN, Debry A, Milinkovitch MC. 2019 Phylogenetic mapping of scale nanostructure diversity in snakes. *BMC Evol Biol* **19**, 91. (doi:10.1186/s12862-019-1411-6)

35. Hazel J, Stone M, Grace MS, Tsukruk VV. 1999 Nanoscale design of snake skin for reptation locomotions via friction anisotropy. *J Biomech* **32**, 477–484. (doi:10.1016/S0021-9290(99)00013-5)

36. Wu W, Yu S, Schreiber P, Dollmann A, Lutz C, Gomard G, Greiner C, Hölscher H. 2020 Variation of the frictional anisotropy on ventral scales of snakes caused by nanoscale steps. *Bioinspir Biomim* **15**, 056014. (doi:10.1088/1748-3190/ab9e51)

37. Rieser JM, Li TD, Tingle JL, Goldman DI, Mendelson JR. 2021 Functional consequences of convergently evolved microscopic skin features on snake locomotion. *PNAS* **118**. (doi:10.1073/pnas.2018264118)

38. Abdel-Aal HA, Vargiolu R, Zahouani H, El Mansori M. 2012 Preliminary investigation of the frictional response of reptilian shed skin. *Wear* **290–291**, 51–60. (doi:10.1016/j.wear.2012.05.015)

39. Abdel-Aal HA. 2018 Surface structure and tribology of legless squamate reptiles. *Journal of the Mechanical Behavior of Biomedical Materials* **79**, 354–398. (doi:10.1016/j.jmbbm.2017.11.008)

40. Benz MJ, Lakhtakia A, Kovalev AE, Gorb SN. 2012 Anisotropic frictional properties in snakes. In *Proceeding of the SPIE*, p. 83390X. San Diego: SPIE. (doi:10.1117/12.916972)

41. Baum MJ, Kovalev AE, Michels J, Gorb SN. 2014 Anisotropic Friction of the Ventral Scales in the Snake Lampropeltis getula californiae. *Tribol Lett* **54**, 139–150. (doi:10.1007/s11249-014-0319-y)

42. Filippov AE, Gorb SN. 2016 Modelling of the frictional behaviour of the snake skin covered by anisotropic surface nanostructures. *Sci Rep* **6**, 23539. (doi:10.1038/srep23539)

43. Dunning J, Patil A, D'Alba L, Bond AL, Debruyn G, Dhinojwala A, Shawkey M, Jenni L. 2023 How woodcocks produce the most brilliant white plumage patches among the birds. *J R Soc Interface* **20**, 20220920. (doi:10.1098/rsif.2022.0920)

44. Burresi M, Cortese L, Pattelli L, Kolle M, Vukusic P, Wiersma DS, Steiner U, Vignolini S. 2014 Bright-White Beetle Scales Optimise Multiple Scattering of Light. *Scientific Reports* **4**, 6075. (doi:10.1038/srep06075)

45. Wilts BD *et al.* 2018 Evolutionary-Optimized Photonic Network Structure in White Beetle Wing Scales. *Adv Mater* **30**, e1702057. (doi:10.1002/adma.201702057)

Acknowledgments

The authors acknowledge useful discussions as well as kind help and support in the lab by Patrick Weiser, Cornelia Pichler, and Weibin Wu. We thank Alfred Wallner and Philippe Wolf for providing the moulted snake skins used for this study. Furthermore, we acknowledge the kind support of Lourance Klose, Tyrone Ping, Yannick Francioli, Daniel Kane (London Zoo), and Nathanel Maury who provided photos of various snakes shown in Figure 1 and the Supplemental.

Funding

This study was supported by the Karlsruhe Nano Micro Facility (KNMF, www.kit.edu/knmf). We acknowledge financial support by the Ministry of Science, Research and the Arts of Baden-Württemberg as part of the sustainability financing of the projects of the Excellence Initiative II. and through the "Ideenwettbewerb Biotechnologie — Von der Natur lernen", Helmholtz Association (MTET Topic 1, 38.01.05) as well as by the German Research Foundation (grant HO2237/12-1).

Data Availability

All photos, SEM and AFM images as well as all optical spectra are available on Dryad Digital Repository https://doi.org/10.5061/dryad.x95x69pw5 Reviewer link: http://datadryad.org/share/BaGuR_ol0juY8RSvPyx8Pe1MmKKQ9eDS6tgkFcg5kR8

Figures

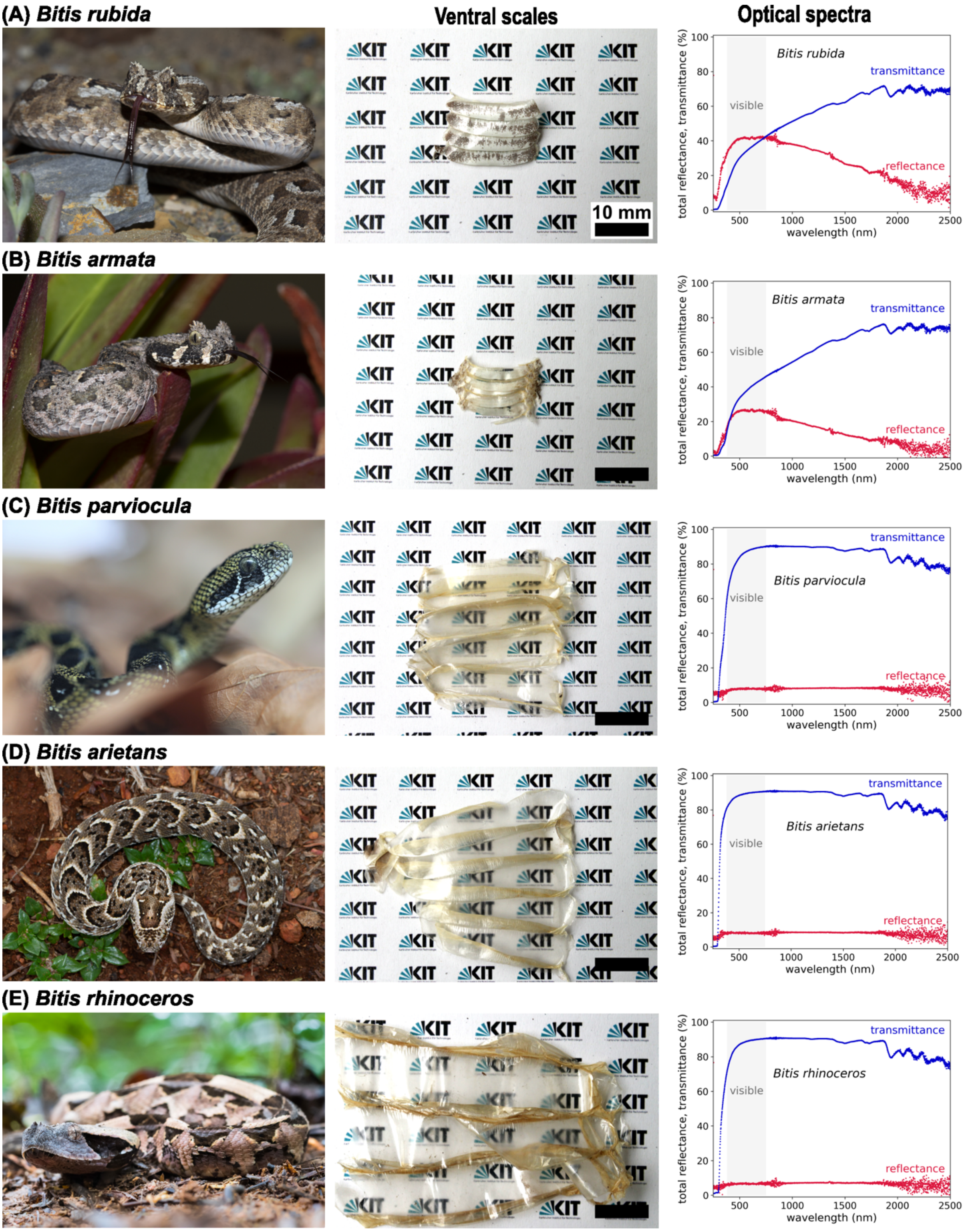

Figure 1: Photographs of the examined snake species of the genus *Bitis* (left), their ventral scales (middle), and respective optical spectra (right) of *B. rubida* (A); *B. armata* (B); *B. parviocula* (C); *B. arietans* (D) and *B. rhinoceros* (E). The white venters of *B. rubida*, *B. armata*, and *B. parviocula* are partly visible in the photographs. The ventral colours of all

snakes are shown and discussed in the Supplemental. All ventral scales were taken from the ventral side of moulted skin and placed on white paper with a print of a university logo (scale bar 10 mm). The printout cannot be read through the scales of *B. rubida* and *B. armata* but is easily spotted through the transparent or translucent scales of *B. parviocula*, *B. arietans*, and *B. rhinoceros*. The optical response of the ventral scales of *B. rubida, B. armata, B. rhinoceros, B. arietans*, and *B. parviocula* is recorded for wavelengths between 250 nm and 2500 nm (right panel). A total reflectance up to 40% and 30% is observed for the white ventral scales of *B. rubida* and *B. armata*, respectively. The total reflectance is largest in the visible range (gray area). However, it gradually decreases for larger wavelengths and finally reduces to 10% for 2500 nm. In opposite to that, the transparent or translucent ventral scales of *B. rhinoceros, B. arietans*, and *B. parviocula* feature an almost constant, low total reflection of 8% over the entire spectrum of consideration. The respective photos of the snakes shown on the left panel are copyrighted by Lourance Klose (*B. rubida, B. armata*), Daniel Kane, (*B. parviocula*), Tyrone Ping (*B. arietans*), and Yannick Francioli (*B. rhinoceros*).

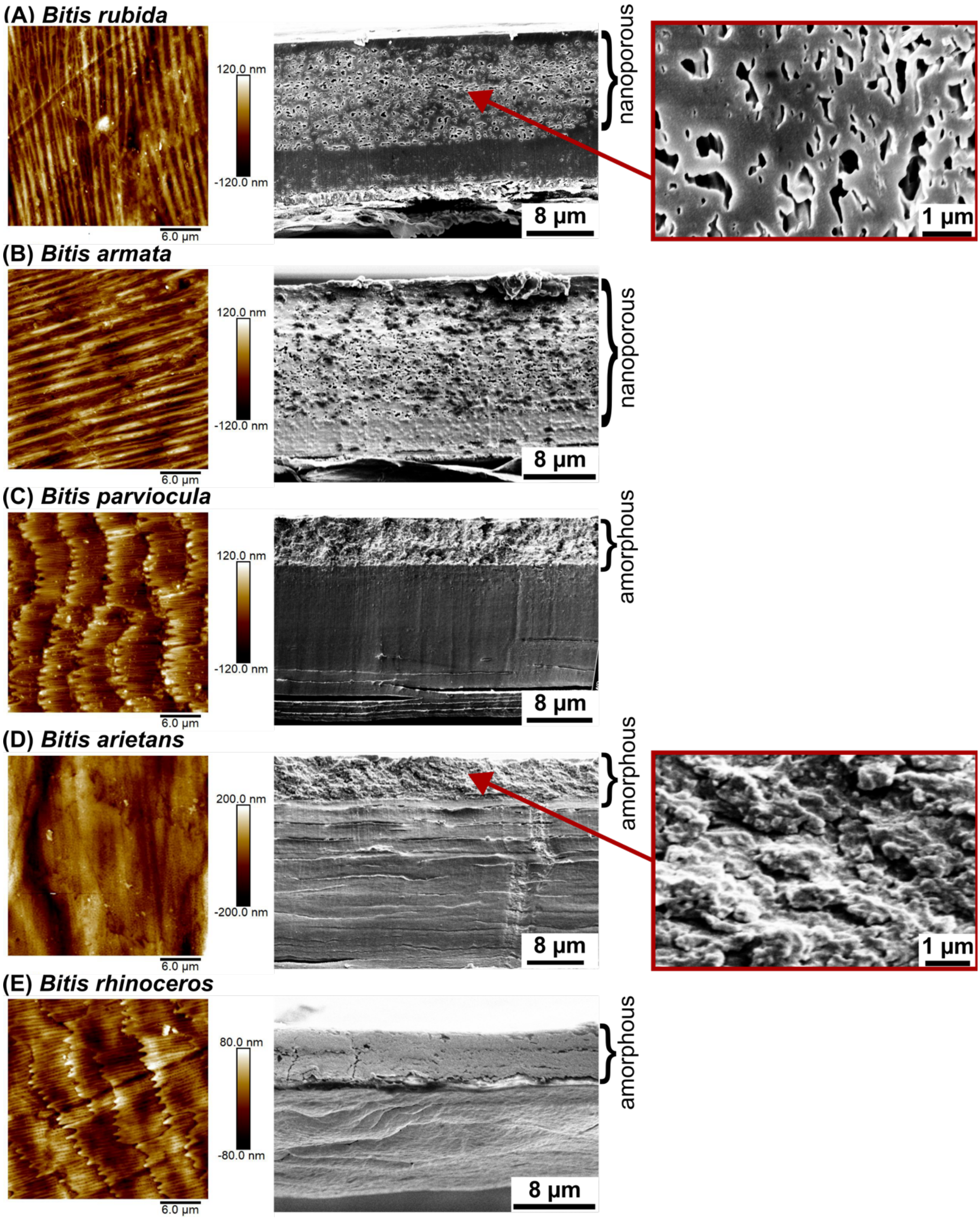

Figure 2: Microstructure of the ventral scales of the five examined *Bitis* species. AFM and SEM images show the surface topography (left) and cross-sections (right) of snake scales of (A) *B. rubida*; (B) *B. armata*; (C) *B. parviocula*; (D) *B. arietans*, and (E) *B. rhinoceros*. A ridge-like surface structure is observed on *B. rubida* and *B. armata*. Microfibril-like structures are found on the ventral scales of *B. parviocula* and *B. rhinoceros*. Numerous pits are detected on

the ventral scales of *B. arietans*. In the cross-section images of scales of *B. rubida* and *B. armata* a spongy structure of nanopores is observed underneath the external surface of the white scales while an amorphous structure without pores is found underneath the transparent or translucent scales of *B. parviocula*, *B. arietans*, and *B. rhinoceros*.